Biochimica et Biophysica Acta 817 (1985) 103–122
Elsevier

BBA 72621

The separate profile structures of the functional calcium pump protein and the phospholipid bilayer within isolated sarcoplasmic reticulum membranes determined by X-ray and neutron diffraction

L. Herbette [a,b,c,*], P. DeFoor [d], S. Fleischer [d], D. Pascolini [a,b], A. Scarpa [a] and J.K. Blasie [a,b]

[a] *Departments of Chemistry and Biochemistry / Biophysics, University of Pennsylvania, Philadelphia, PA 19104,* [b] *Department of Biology, Brookhaven National Laboratory, Upton, NY 11973,* [c] *Departments of Medicine and Biochemistry, University of Connecticut, Farmington, CT 06032 and* [d] *Department of Molecular Biology, Vanderbilt University, Nashville, TN 37235 (U.S.A.)*

(Received October 19th, 1984)
(Revised manuscript received March 11th, 1985)

Key words: Ca^{2+} pump protein; Phospholipid bilayer; Electron density profile; Sarcoplasmic reticulum; X-ray diffraction; Neutron diffraction

The detailed profile structure of the isolated sarcoplasmic reticulum membrane was studied utilizing a combination of X-ray and neutron diffraction. The water and lipid profile structures within the sarcoplasmic reticulum membrane were determined at 28 Å resolution directly by neutron diffraction and selective deuteration of the water and lipid components. The previously determined electron density profile structure of the sarcoplasmic reticulum membrane at 12 Å resolution was subjected to model refinement analysis constrained by the neutron diffraction results, thereby providing unique higher resolution calculated lipid and protein profile structures. It was found that the lipid bilayer profile structure of the isolated sarcoplasmic reticulum membrane is asymmetric, primarily the result of more lipid residing in the inner versus the outer monolayer of the sarcoplasmic reticulum lipid bilayer. The asymmetry in the lipid composition was necessarily coincident with a complimentary asymmetry in the protein mass distribution between the two monolayers in order to preserve the overall cross-sectional area of lipid and protein throughout the lipid bilayer region of the sarcoplasmic reticulum membrane profile structure. Approximately 50% of the mass of the total protein was found to be localized externally to the sarcoplasmic reticulum membrane lipid bilayer protruding from the outer lipid monolayer into the extravesicular medium. The structural features of the protein protrusion appear to be rather variable depending upon the environment of the sarcoplasmic reticulum membrane. This highly asymmetric structural organization of the sarcoplasmic reticulum membrane profile is consistent with its primary function of unidirectional calcium transport.

Introduction

The sarcoplasmic reticulum membrane has been the subject of numerous investigations on both functional and structural levels. The functional studies of this membrane have provided a detailed, though still incomplete, mechanism for the unidirectional transport of calcium across the sarcop-

* To whom all correspondence should be addressed at (present address): University of Connecticut Health Center, Department of Medicine, Farmington, CT 06032, U.S.A.

Abbreviation: Hepes, 4-(2-hydroxyethyl)-1-piperazineethanesulfonic acid.

lasmic reticulum membrane permeability barrier upon hydrolysis of an energy source such as ATP (for reviews, see Refs. 1–4). This biochemical mechanism has been supplemented with extensive studies on the morphology and ultrastructure of the sarcoplasmic reticulum membrane, all indicating an asymmetric membrane profile (or cross-sectional) structure. Freeze-fracture electron microscopy of isolated sarcoplasmic reticulum has demonstrated an asymmetric distribution of particles which reside predominantly in the outer concave fracture face corresponding to the outer monolayer of the closed sarcoplasmic reticulum vesicle (cytosolic side) with the inner convex fracture face being relatively particle free [5,6]. Negative-staining electron microscopy has revealed projections presumed to be protein at the extravesicular surface of the closed sarcoplasmic reticulum vesicle [7] consistent with the thin-section electron microscopic images of the sarcoplasmic reticulum membrane [8–10]. Although electron microscopy may provide some information regarding the basic structural features of the functional sarcoplasmic reticulum membrane, internal inconsistencies also exist such as the particle area density discrepancy between negative stain and freeze-fracture images of the sarcoplasmic reticulum membrane [11].

The profile structure of the functional sarcoplasmic reticulum membrane has been investigated utilizing lamellar X-ray diffraction at a relatively low resolution of approx. 17 Å [12,13] and at somewhat higher resolution of approx. 11 Å [14,15]. These studies have shown that the sarcoplasmic reticulum membrane electron density profile is highly asymmetric with the major protein, the calcium pump (Ca^{2+} and Mg^{2+} sensitive ATPase), probably spanning the lipid bilayer. The higher resolution electron density profile contains electron dense features outside of the phospholipid headgroup region at the extravesicular surface of the sarcoplasmic reticulum membrane, believed to be protein [14]. Attempts have been made to determine the protein contribution to the sarcoplasmic reticulum membrane profile structure by employing X-ray solution scattering techniques on both partially delipidated sarcoplasmic reticulum membranes [16] and detergent solubilized sarcoplasmic reticulum protein [17]. X-ray and neutron diffraction studies of reconstituted sarcoplasmic reticulum [18,19] have allowed some information to be obtained regarding the separate contribution of protein and lipid to the total profile structure of this membrane system although this approach is somewhat problematic in this case due to some loss in the unidirectionality of the pump protein in these particular reconstituted preparations. The 'in-plane' structure of the sarcoplasmic reticulum membrane was previously examined utilizing equatorial X-ray diffraction providing a limited amount of structural information whose interpretation remains incomplete [12,13]. Optical diffraction of freeze-fracture electron microscopic images suggest that the calcium pump protein may be organized in a weak lattice of calcium pump dimers in the sarcoplasmic reticulum membrane plane [20], consistent with target inactivation analysis which also supports the dimer model [21].

In this paper, we have employed X-ray and neutron diffraction techniques to directly decompose the electron density profile structure of the isolated sarcoplasmic reticulum membrane into the separate profile structures for water, lipid and protein at approx. 11 Å resolution. It is shown that the calcium pump protein spans the membrane lipid bilayer in contact with both the intravesicular and extravesicular water spaces with a major portion protruding substantially into the extravesicular water space. The membrane lipid and water profiles are asymmetric consistent with the complimentary asymmetry in the protein mass distribution within the lipid bilayer region of the sarcoplasmic reticulum membrane profile structure. Our results indicate that the protein protrusion from the extravesicular surface of the sarcoplasmic reticulum membrane profile may be somewhat 'elastic' with dimensions dependent upon the environment of the sarcoplasmic reticulum vesicle. These structural results pertain to the fully functional, isolated sarcoplasmic reticulum membrane as shown by our previous studies [14,46]. We have previously reported brief summaries of this work [19,22].

Methods

(i) Sarcoplasmic reticulum preparation and assays

Sarcoplasmic reticulum vesicles were isolated from rabbit white (fast) back and hind leg muscle,

purified by zonal density gradient centrifugation and suspended in a solution containing 300 mM sucrose, 100 mM KCl, 1 mM Hepes (pH 7.1) [23]. The suspension was quickly frozen in liquid nitrogen and stored at −70°C until use. The sarcoplasmic reticulum vesicles were further subfractionated into light and heavy sarcoplasmic reticulum. The light sarcoplasmic reticulum vesicles, which were devoid of electron dense compartmental contents, were used in these studies [24]. Lipid was extracted from isolated sarcoplasmic reticulum vesicles with chloroform/methanol (2:1, v/v) [25] and dried under nitrogen. Protein concentrations of the samples were determined by the method of Lowry et al. [26], using bovine serum albumin as a standard. Phospholipid phosphorus was estimated from a determination of the total phosphorus content according to Meissner and Fleischer [27]. The lipid to protein (L/P) ratio is expressed as μg phosphorus per mg protein.

(ii) Sarcoplasmic reticulum deuteration methods

(a) Biosynthetic deuteration of sarcoplasmic reticulum lipids. White New Zealand rabbits (1.5 kg) were fed a diet supplemented with 10–20 mg of deuterated sodium acetate per day for six weeks. Deuterated acetic acid was neutralized to pH 7.0 and concentrated solutions (2–4 M) of sodium acetate were mixed with rabbit chow which was allowed to dry overnight. Control experiments involved supplementing the diet with protonated sodium acetate. Sarcoplasmic reticulum vesicles were isolated as described [14,23] and phospholipids were extracted [25] from this highly purified fraction of sarcoplasmic reticulum vesicles. Proton Fourier transform NMR (FT-NMR) spectra were obtained from this lipid extract in chloroform and compared to fully protonated sarcoplasmic reticulum lipid controls. A relatively long delay time between FT-NMR pulses of approx. 10 s was employed in order to quantitatively compare these spectra. The percent of total deuteration in the sarcoplasmic reticulum lipids was estimated to be 50–60% from the reduction in total integrated intensity of the partially deuterated sarcoplasmic reticulum lipid sample. Since the entire spectrum from the deuterated sarcoplasmic reticulum lipid sample was uniformly reduced in intensity, no preferential deuteration of any portion of the phospholipid molecules in the entire sarcoplasmic reticulum lipid population had taken place. Thus approx. 50–60% of the sarcoplasmic reticulum lipid mixture was perdeuterated before exchange into normally protonated sarcoplasmic reticulum vesicles.

(b) Phospholipid exchange methods *. PC and PE extracted from both the perdeuterated sarcoplasmic reticulum lipid mixture and fully protonated sarcoplasmic reticulum lipids were exchanged into fully protonated purified sarcoplasmic reticulum vesicles utilizing a non-specific lipid transfer protein * [28–30]. In early experiments, a phosphatidylcholine specific transfer protein was also used [31,32]. A 7-fold (relative to the amount of membrane phospholipid, see below) excess of either deuterated or protonated sarcoplasmic reticulum lipids was suspended in 300 mM sucrose, 1 mM Hepes (pH 7.1) and sonicated briefly at low power to form liposomes. The solution was sonicated until it clarified and centrifuged (40000 × *g*, 30 min) to remove the larger lipid aggregates. Lipid transfer proteins were isolated from bovine liver and purified [28]. The lipid (240 μg/ml) was added to a reaction mixture containing 1 mM Hepes, 0.004% azide, 0.06 M sucrose followed by addition of the phospholipid transfer protein (100 μg/ml). Sarcoplasmic reticulum membrane vesicles (24 μg phosphorus/mg protein in 1 ml) were added to this reaction mixture and incubated for various times (1–5 h) at 30°C. The exchange reaction was allowed to proceed so that, under the conditions of the assay, nearly all the lipid in the outer monolayer of the sarcoplasmic reticulum membrane was replaced with PC and PE (see Results). These lipid exchanged sarcoplasmic reticulum membrane vesicles were purified by a sucrose step-density gradient so that the exchanged sarcoplasmic reticulum membrane vesicles were separated from liposomes. The time-course for lipid exchange [30,32] into sarcoplasmic re-

* The specific phosphatidylcholine transfer protein is specific for exchanging phosphatidylcholine in the presence of other lipid species. The more general lipid transfer protein, designated nonspecific lipid transfer protein, has broader phospholipid specificity and was used to exchange both PC and PE.

ticulum vesicles * and details of the exchange reactions were monitored in separate reaction mixtures and are described elsewhere.

(iii) Electron microscopy of sarcoplasmic reticulum vesicles

Isolated sarcoplasmic reticulum vesicles were fixed by the tannic acid-OsO_4 method previously described [10]. Thin sections were cut on an LKB Ultratome (LKB Instruments, Inc., Rockville, MD) with diamond knives (E.I. DuPont de Nemours and Co., Wilmington, DE), and subsequently examined in a Hitachi HU-11b electron microscope (Tokyo, Japan). Freeze-fracture microscopy of exchanged sarcoplasmic reticulum was carried out as described previously [25].

(iv) Assays of sarcoplasmic reticulum function

Ca^{2+} loading and ATPase activity of sarcoplasmic reticulum vesicles in the presence of oxalate, which forms a precipitate of calcium oxalate inside the vesicles, were measured under similar conditions, as previously described [24]. The amount of Ca^{2+} taken up by sarcoplasmic reticulum in the first 1 min interval, i.e. where the reaction kinetics are linear with time, represents the Ca^{2+} loading rate expressed as μmol Ca^{2+}/mg per min. The Ca^{2+} accumulation in a 10-min interval is defined as the loading capacity. The Ca^{2+} loading efficiency is the ratio of the Ca^{2+} loading rate to the Ca^{2+}-stimulated ATPase activity rate (μmol P_i/mg per min), both assayed under similar conditions.

(v) X-ray and neutron diffraction methods: data collection, reduction and phasing

Exchanged sarcoplasmic reticulum vesicles were thawed and resuspended in 100 mM KCl, 10 μM Tris maleate (pH 7.0) and oriented membrane multilayers were prepared for X-ray and neutron diffraction studies as described [14]. Membrane multilayers were equilibrated at 93% relative humidity under gas-flow conditions [14] for X-ray diffraction studies and 88% relative humidity under sealed conditions [18] for neutron diffraction studies at 7–8°C; for the latter studies, the saturated salt solutions utilized were prepared at 100% ^2H_2O and a 75% $^2H_2O/H_2O$ ratio allowing partial dehydration and H_2O-^2H_2O exchange of the samples to be carried out simultaneously.

For lamellar X-ray diffraction experiments, the equipment design, specimen geometry, data acquisition and data reduction were previously described in detail [14]. Lamellar neutron diffraction data were collected at the high flux beam reactor using the Brookhaven low-angle diffractometer operating at 2.36 Å. Equipment design, specimen geometry, data acquisition and data reduction for neutron diffraction experiments have been described in detail [15]. In the case of neutron diffraction studies, the lamellar background scattering was calculated as described by Pachence et al. [33].

The lamellar diffraction (X-ray and neutron) from oriented sarcoplasmic reticulum membrane multilayers exhibited a considerable degree of lattice disorder. The continuous X-ray lamellar intensity function was phased by a direct deconvolution procedure which takes into account multilayer lattice disorder [34] and multilayer unit cell electron density profiles were calculated as previously described [14]. The continuous neutron lamellar intensity functions were likewise phased by a similar analysis. Alternatively, the lamellar neutron reflections were integrated by fitting Gaussian curves to the maxima in the lamellar data and these integrated reflections were phased by the swelling method [35] using a previously published algorithm [36]. The phase assignments for the neutron diffraction data were identical using either the direct deconvolution procedure or the swelling method. All neutron scattering contrast profiles for the multilayer unit cell were determined by the appropriate Fourier series utilizing the phased integrated lamellar reflections according to Guinier (Ref. 37, see also Ref. 33). Appropriate neutron scattering profiles were scaled to one another [38] and difference profiles were calculated as unit cell water profile structures utilizing H_2O-^2H_2O exchange, and unit cell lipid profile structures utilizing protonated versus deuterated sarcoplasmic reticulum lipids.

* Further details of the lipid exchange methodology as applied to the sarcoplasmic reticulum membrane and the time-course for lipid exchange into the sarcoplasmic reticulum membrane, are described in a manuscript recently submitted by Lunardi, J., DeFoor, P. and Fleischer, S.

(vi) Model refinement methods

Neutron diffraction. Difference unit cell neutron scattering profiles calculated from sarcoplasmic reticulum with protonated versus deuterated lipid in the neutron diffraction study directly provided the lipid profile structure within the isolated sarcoplasmic reticulum membrane where the multilayer unit cell profile contains two apposed single membrane profiles as previously shown [14]. These low resolution (28 Å) lipid profile structures were analyzed by fitting a step-function model containing 5 steps per single membrane profile within the unit cell difference profile in order to quantitatively allow for transform truncation errors. The fitting procedure consisted of Fourier transforming an initial step-function model profile once to provide the model's structure factor and subsequently Fourier transforming this structure factor (at the resolution of the experimental data of 28 Å) to generate a continuous, calculated unit cell difference profile $\Delta\rho_c(x)$ equivalent to the step-function model; the model was then refined against the experimental unit cell difference profile $\Delta\rho_e(x)$ until the normalized least-squares fit of

$$\int_{-D/2}^{+D/2}[\Delta\rho_c(x)-\Delta\rho_e(x)]^2\,dx \Big/ \int_{-D/2}^{+D/2}[\Delta\rho_e(x)]^2\,dx$$

(where D is the unit cell profile dimension) was better than 1%. The step-function model thus fitted could be used to estimate the number of lipid molecules for each monolayer of the sarcoplasmic reticulum membrane bilayer by taking into account the measured lipid to protein ratio equal to 128 mole phospholipid per mole calcium pump protein [15]. A similar procedure was used to estimate the ratio for the amount of water hydrating the inner versus outer phospholipid headgroup region of the sarcoplasmic reticulum membrane lipid bilayer. For these calculations, a step-function model containing 6 steps per membrane was fitted to the experimental difference unit cell profile (28 Å resolution) obtained by the H_2O-^2H_2O exchange of the protonated sarcoplasmic reticulum membrane used in the above study. This procedure provided a measure of the relative amounts of water within the two phospholipid headgroup regions of the membrane profile exclusive of the 'pure' water layer in the vicinity of $x = 0$ Å of the unit cell profile structure, i.e., between the phospholipid headgroups of the two apposed membranes of the collapsed sarcoplasmic reticulum vesicle designated as the intravesicular water space. Both the phospholipid bilayer asymmetry and the relative amounts of water in the two phospholipid headgroup regions within the sarcoplasmic reticulum membrane profile could be determined with an accuracy of $\pm 1\%$ (S.D.) based on this procedure.

X-ray diffraction. The electron density profile structure of the sarcoplasmic reticulum membrane at approx. 13 Å resolution was then subjected to the following detailed analysis utilizing pertinent information from the neutron diffraction study in order to obtain the separate higher-resolution lipid and protein profile structures within the sarcoplasmic reticulum membrane.

The experimental electron density profile for the symmetric lipid bilayer of pure sarcoplasmic reticulum lipids at 15 Å resolution [15] was fitted with a step-function model profile in which 5 steps defined the lipid bilayer and 2 steps represented the water layers at either surface of the bilayer. The experimental unit cell electron density profile for the isolated sarcoplasmic reticulum membranes at 13 Å resolution was fitted with a step-function model profile in which 10 steps defined the membrane and 2 steps represented water layers at either membrane surface. As for neutron diffraction studies, the fits resulting from the refinement of these model profiles were obtained to less than 5% normalized least-squares deviation between the experimental profile and the doubly-Fourier transformed step-function model profile structures.

The resulting step-function model profile for sarcoplasmic reticulum lipids was placed on an absolute electron density scale by calculating the electron density for each of the 5 steps within the model using the known composition of the lipid mixture and electron densities of lipid components based on other studies [33,39,40]. The calculated values of 0.430 $e/Å^3$ for the phospholipid headgroup steps, 0.296 $e/Å^3$ for the hydrocarbon chain $(CH_2)_n$ steps and 0.232 $e/Å^3$ for the chain terminal methyl group step were used. This scale so constructed for the bilayer of isolated sarcoplasmic reticulum lipids was deemed reasonable since the water spaces between bilayers were then

found to have an electron density value of 0.334 $e/Å^3$ in the refined step-function model, as expected.

The absolute electron density scale for the step-function model of the sarcoplasmic reticulum membrane profile was constructed based on information abstracted from both the lipid and water profile structures obtained directly by neutron diffraction. In order to best utilize the neutron diffraction results, model refinement calculations were employed which utilized linear combinations of water, lipid and protein computed for each step of the sarcoplasmic reticulum membrane profile structure.

The model refinement was based on the following calculated and experimental parameters:

(1) A measured lipid to protein ratio of approx. 26 μg phosphorus per mg protein which, using 119000 for the molecular weight of the calcium pump protein which is approx. 90% of the total protein, yields 128 mole phospholipid per mole calcium pump protein.

(2) An average electron density of 0.405 $e/Å^3$ was calculated for the calcium pump protein based on the amino acid composition [41] and the electron densities of the amino acids [42].

(3) The average cross sectional area of a phospholipid molecule in the liquid-crystalline state under the conditions of hydration for the sarcoplasmic reticulum membrane utilized in the diffraction studies was assumed to be approx. 60 $Å^2$ [40].

(4) The average electron density for the phospholipid headgroups and fatty acyl chains obtained for the bilayer of extracted sarcoplasmic reticulum lipids were assumed to be applicable to the phospholipid molecules in the sarcoplasmic reticulum membrane.

The model refinement was further constrained to predict:

(1) The measured asymmetry in the numbers of phospholipid molecules between the outer and inner monolayers of the sarcoplasmic reticulum membrane bilayer, a parameter directly obtained in the neutron diffraction study.

(2) The measured ratio for the amount of water hydrating the two phospholipid headgroup regions of the sarcoplasmic reticulum membrane bilayer, a parameter directly obtained in the neutron diffraction study.

Thus, the electron density scale for the step-function model profile was systematically varied until appropriate linear combinations of water, lipid and protein computed for each step predicted the same values for the phospholipid bilayer asymmetry and the asymmetry in the water hydrating the headgroups of the phospholipid bilayer within the sarcoplasmic reticulum membrane profile structure as determined experimentally from the neutron diffraction study. The electron density scale could be determined uniquely with an accuracy of better than $\pm 2\%$ (S.D.) using this procedure.

With the correct electron density scale for the sarcoplasmic reticulum membrane profile established by this model refinement procedure, the protein profile for the sarcoplasmic reticulum membrane was also thereby uniquely generated at 13 Å resolution. It should be emphasized here, that in a model refinement of an electron density profile, the basic assumption is that the profile can be decomposed into its separate lipid and protein profile structures assuming that the protein has either an average area or an average electron density throughout the membrane profile. In these cases, only the corresponding electron density profile or the area profile * structures of the protein can be calculated. With these reservations, the model refinement analysis of the electron density profile for the sarcoplasmic reticulum membrane was performed above assuming that the calculated average electron density of 0.405 $e/Å^3$ for the protein was constant throughout the membrane profile.

A final additional constraint was then employed for the model refinement procedure, namely the conservation of the total cross-sectional area of protein, lipid and water from step to step along the profile axis. It was found that when a constant average electron density (0.405 $e/Å^3$) for the protein was used, the total cross sectional area for the lipid, water and protein within each step varied somewhat in the refined model profile. From this model profile, an average total cross sectional area along the extent of the membrane profile could be

* The area occupied by the protein in the membrane plane as a function of the profile coordinate.

calculated. Again, linear combinations of water, lipid and protein were computed for each step subject to the constraints described above, but this time bounded by the calculated average total cross sectional area allowing the electron density of the protein to vary slightly along the profile axis. Thus a further refined area profile for the protein was computed by relaxing somewhat the constraint of a constant electron density for the protein to allow the total cross sectional area of all membrane components to remain constant throughout the membrane profile. The preservation of the total cross sectional area along the membrane profile axis and the slightly varying electron density of the protein were deemed to be a more physically reasonable model. The resulting step-function lipid, protein and water profile structures were doubly Fourier transformed to provide their respective continuous separate profile structures which were fully consistent with the original continuous electron density profile for the sarcoplasmic reticulum membrane.

(vii) X-ray scattering of sarcoplasmic reticulum vesicles

X-ray scattering data were obtained from unilamellar vesicular dispersions of sarcoplasmic reticulum (1–10 mg/ml) utilizing a one-dimensional position-sensitive X-ray detector [14]. The background scattering was obtained from the buffer solution only. The spherically symmetric intensity function (corrected for background scattering) was also appropriately corrected by $S^2 = (2 \sin \theta/\lambda)^2$ and the autocorrelation function $Q_{exp}(x)$ for the membrane profile was obtained by Fourier transformation of this corrected intensity function.

Fluctuations in $Q_{exp}(x)$ which appeared to be significant in magnitude were analyzed in order to determine the maximal width of the sarcoplasmic reticulum membrane profile in vesicular dispersions. This analysis of $Q_{exp}(x)$ was performed at two levels. For the first level of refinement, the step-function model that was fitted to the experimental electron density profile structure obtained from X-ray diffraction of sarcoplasmic reticulum membrane multilayers (see section vi) was used as a starting point. For this calculation only the single membrane profile within $0 \leqslant x \leqslant D/2$ of the unit cell profile was used. The step-function model to the experimental single membrane profile contained within $0 \leqslant x \leqslant D/3$, which corresponds to the lipid bilayer region of the sarcoplasmic reticulum membrane profile structure, was kept constant and the extent of the electron dense region within $D/3 \leqslant x \leqslant D/2$ was varied. These model profile structures were then subjected to the convolution operation ($*$) such that

$$Q_{cal}(x) = \rho_{sm}(x) * \rho_{sm}(-x)$$

where $Q_{cal}(x)$ is the calculated autocorrelation function for the single membrane profile, $\rho_{sm}(x)$. These calculated autocorrelation functions were compared to the experimentally obtained single membrane autocorrelation function $Q_{exp}(x)$ and a best-fit was obtained for the variation described above. The second level of refinement involved small changes in the step-function model profile within the lipid bilayer region ($0 \leqslant x \leqslant D/3$) of the sarcoplasmic reticulum membrane profile. A small change of less than 5% in the total width of this region of the profile structure yielded a significantly better fit of $Q_{cal}(x)$ to $Q_{exp}(x)$. The overall best-fit within experimental error of $Q_{cal}(x)$ to $Q_{exp}(x)$ was thus obtained by this refinement procedure.

Finally, a calculation was performed to test for possible contributions of intermembrane correlations (arising from vesicle-vesicle contact) to the experimental $Q_{exp}(x)$ function (see Fig. 1). The best-fit step-function model profile for the sarcoplasmic reticulum membrane in dispersion obtained by the above procedure $\rho_e(x)$ was now used to construct a membrane-pair profile composed of two apposing single membrane profiles as shown in Fig. 1. The two apposing membrane profiles were allowed to overlap by Δ in the region containing protein protrusions from the membrane surface and for each model thus generated, an autocorrelation function $Q'_{cal}(s)$ was calculated. Weighted averages of each $Q'_{cal}(x)$ for a particular Δ value and $Q_{cal}(x)$ were generated according to $Q''_{cal}(x) = xQ_{cal}(x) + (1 - x)Q'_{cal}(x)$ and least-squares fits of $Q''_{cal}(x)$ to $Q_{exp}(x)$ were obtained. It was thereby determined that for the various possible degrees of overlap in the protruding protein region investigated, there must be less than a 5% contribution of the intermembrane correlations to the experimental function $Q_{exp}(x)$.

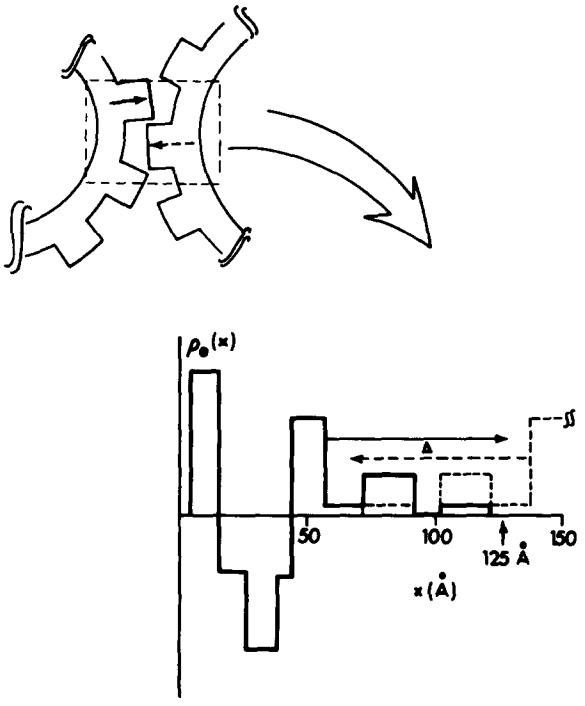

Fig. 1. Two apposed step-function model profiles $\rho_e(x)$ for the sarcoplasmic reticulum membrane were allowed to overlap by Δ in the region containing the protein protrusions from the extravesicular surface of the membrane lipid bilayer. The resulting membrane-pair model profiles were used in the calculations of the autocorrelation functions $Q'_{cal}(x)$. (See text for details).

(viii) Materials

Glutaraldehyde (vacuum distilled and treated to remove traces of glutaric acid) was obtained from Polysciences, Inc. (Paul Valley Industrial Park, Warrington, PA). Epon 812 and OsO_4 were purchased from Polysciences, Inc. Tannic acid and uranyl acetate were obtained from Mallinckrodt Inc. (St. Louis, MO). Deuterated acetic acid was purchased from Sigma Chemical Co. (St. Louis, MO).

Results

(i) Properties of exchanged sarcoplasmic reticulum

The time-course of phospholipid exchange from liposomes into sealed sarcoplasmic reticulum vesicles utilizing both a specific [32] and a non-specific * [29,30] transfer protein has been described in detail. The reaction is characteristically biphasic with $40 \pm 5\%$ of the phospholipid in the sarcoplasmic reticulum being exchanged relatively rapidly within 1–2 hours followed by a slower incorporation of additional lipid, with a maximum, lipid species-dependent half-time of about 1 day. Since our sarcoplasmic reticulum vesicle preparations are tightly sealed with a high coupling efficiency for ATP-energized Ca^{2+} accumulation (see Table I and Refs. 23 and 25), it would appear that the phospholipid exchange reaction initially involves the outer monolayer of the sarcoplasmic reticulum lipid bilayer which, as expected, should be relatively fast. The slower rate of exchange is interpreted to represent exchange into the inner monolayer of the membrane bilayer which appears to be rate limited by the transbilayer migration ('flip-flop') rate. This biphasic reaction therefore suggests that approx. 40% of the total phospholipid in the sarcoplasmic reticulum membrane may reside in the outer monolayer with the remainder making up the inner monolayer of the sarcoplasmic reticulum membrane lipid bilayer. Pertinent to these studies, the exchanged sarcoplasmic reticulum membrane samples were analyzed by X-ray and neutron diffraction more than two days after the exchange procedure. This means that 'flip-flop' of exchanged lipid within the sarcoplasmic reticulum membrane should have reached equilibrium so that the lipid profile structure within the sarcoplasmic reticulum membrane as obtained by neutron diffraction methods represents the normal, time-averaged lipid distribution within the sarcoplasmic reticulum membrane bilayer.

Table I summarizes the functional properties of phospholipid exchanged sarcoplasmic reticulum. The lipid to protein ratio of sarcoplasmic reticulum exchanged with either a specific phosphatidylcholine or non-specific transfer protein is very similar to that of non-exchanged sarcoplasmic reticulum. Even though under these conditions the lipid to protein ratios of the protonated and deuterated lipid exchanged sarcoplasmic reticulum are slightly higher than controls for the non-specific transfer protein, they were very similar to each other making them a good pair for the neutron diffraction study. The calcium loading efficiency ratios for the lipid exchanged sarcoplasmic reticulum were in the same range as for non-exchanged

* See footnote on p. 105.

TABLE I

FUNCTIONAL CHARACTERISTICS OF PHOSPHOLIPID-EXCHANGED SARCOPLASMIC RETICULUM (SR)

Sample	Non-exchanged SR	901-5A	901-5B	433D	433N
SR lipids		deuterated total lipids	protonated total lipids	deuterated PC & PE	protonated PC & PE
Transfer protein	–	PC-specific	PC-specific	non-specific	non-specific
Phospholipid/protein (μmol P_i/mg protein)	23.6	23.7	22.1	25.1	26.5
Ca^{2+} loading rate (μmol Ca^{2+}/mg per min)	3.60	3.46	3.16	2.46	3.19
Ca^{2+} loading capacity (μmol Ca^{2+}/mg per 10 min)	9.27	7.93	7.32	7.24	7.60
Ca^{2+} stimulated ATPase (μmol P_i/mg per min)	1.59	1.60	1.46	1.67	1.57
Ca^{2+} loading efficiency (Ca^{2+}/ATP)	2.2	2.2	2.2	1.5	2.0

sarcoplasmic reticulum. In Fig. 2, freeze-fracture electron microscopy of sarcoplasmic reticulum exchanged with protonated (Fig. 2A) and deuterated (Fig. 2B) sarcoplasmic reticulum lipids shows that the membrane particle distributional asymmetry between concave and convex faces has not been altered since it is very similar to freeze-fracture images of sarcoplasmic reticulum which were not exchanged (Fig. 2C). Finally, the electron density profile structure of exchanged sarcoplasmic reticulum at 10 Å resolution was found to be very similar to that of non-exchanged sarcoplasmic reticulum previously reported (Ref. 14, data not shown).

(ii) Lipid and water profile structures of isolated sarcoplasmic reticulum obtained directly by neutron diffraction

Lamellar neutron diffraction was obtained from partially hydrated oriented multilayers of sarcoplasmic reticulum exchanged with protonated versus perdeuterated (Fig. 3A) sarcoplasmic reticulum phospholipids using the non-specific lipid transfer protein in two separate exchange experiments. A typical experiment with a unit cell profile dimension of $D = 170$ Å for sarcoplasmic reticulum exchanged with the non-specific lipid transfer protein (PC + PE only) exhibited significant changes particularly in the first-order $I(h = 1)$ and the sixth-order $I(h = 6)$ lamellar reflections upon deuteration of the sarcoplasmic reticulum lipid.

The difference unit cell profile calculated from the scaled intensity functions as derived from Fig. 3A corresponds strictly to the exchanged phospholipid profile within the sarcoplasmic reticulum membrane and is shown in Fig. 4A. This profile actually represents the total lipid profile of the sarcoplasmic reticulum membrane (since PC and PE are the dominate lipid species in the membrane and the neutron diffraction experiments were carried out following equilibration for 'flip-flop' of exchanged phospholipid across the membrane profile) and thereby provides the distribution of lipid between both monolayers of the normal sarcoplasmic reticulum membrane lipid bilayer. The water profile structure is shown in Fig. 4B for comparison and was obtained from $H_2O/^2H_2O$ exchange of the deuterated (lipids) sarcoplasmic reticulum multilayer at $D = 170$ Å.

The asymmetry in the lipid profile structure is evident in the difference between neutron scattering densities for the phospholipid headgroups of the sarcoplasmic reticulum bilayer in Fig. 4A. The area under each maximum within the difference profile of Fig. 4A was obtained quantitatively as described in the Methods. The results indicate that approximately $54 \pm 1\%$ (mean $\pm$ S.D.) of the phospholipid is located in the inner versus the outer

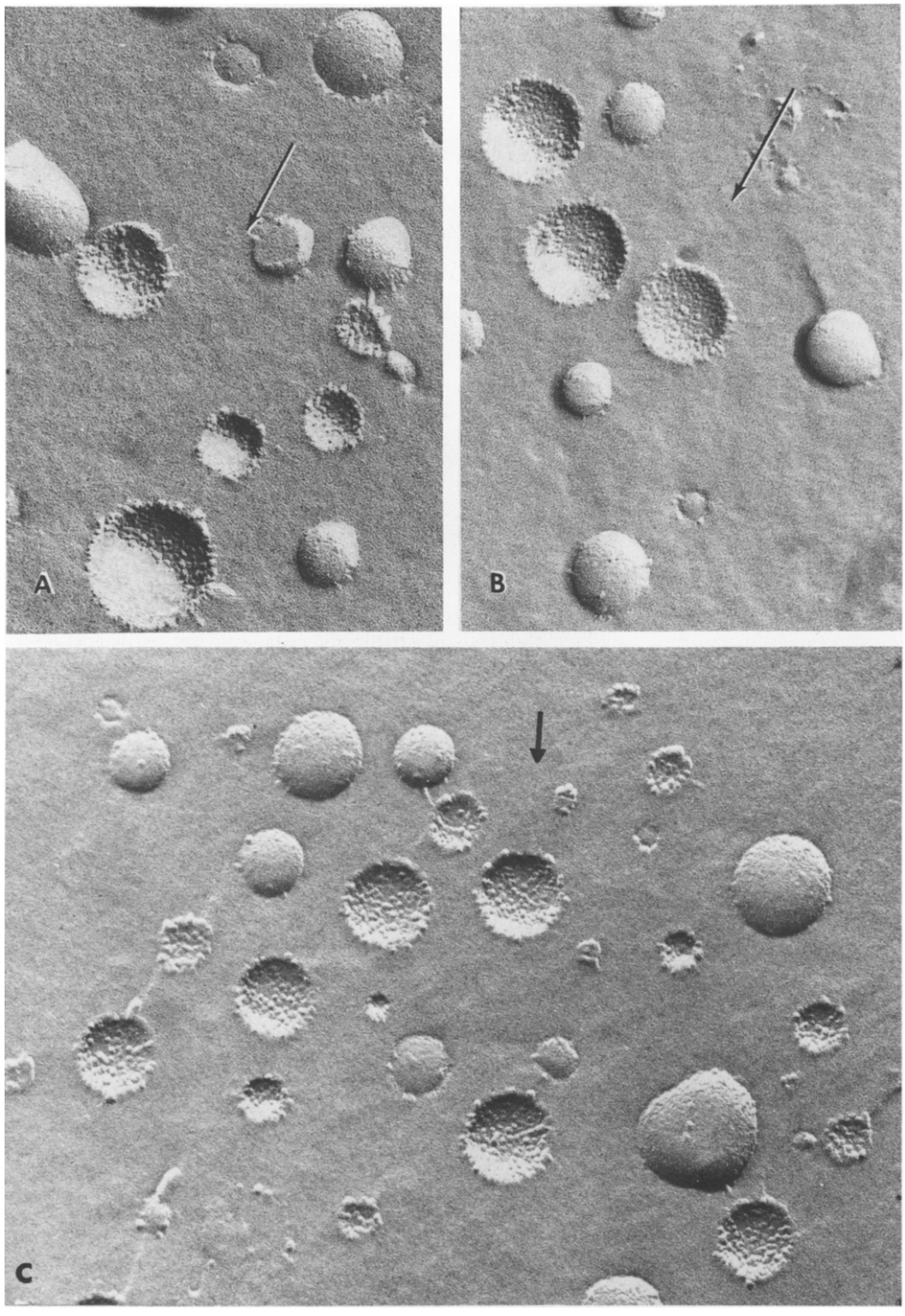

Fig. 2. Freeze-fracture electron micrographs of sarcoplasmic reticulum exchanged (non-specific transfer protein) with protonated (A) and deuterated (B) sarcoplasmic reticulum phospholipids and (C) non-exchanged sarcoplasmic reticulum. Note that in each case, the particles are asymmetrically distributed, occurring mostly in the outer (concave) fracture faces. The arrows indicate the direction of shadowing.

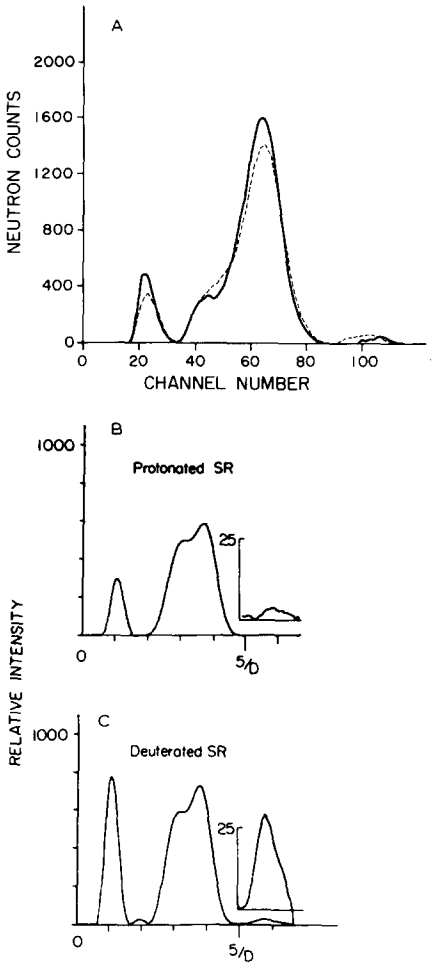

Fig. 3. (A) Lamellar neutron diffraction from oriented sarcoplasmic reticulum (SR) membrane multilayers hydrated with 100% ^2H_2O is shown. Sarcoplasmic reticulum membranes were prepared to contain either protonated (solid line) or perdeuterated (dashed line) sarcoplasmic reticulum lipids (phosphatidylcholine and phosphatidylethanolamine) incorporated via an exchange reaction catalyzed by the non-specific transfer protein. The relative diffracted intensities have been numerically smoothed and appropriately corrected for lamellar background scattering and geometric considerations, but have not been scaled to one another (see text). The lamellar intensity functions are characteristic for sarcoplasmic reticulum membrane multilayers possessing a considerable degree of lattice disorder [14]. Note the strong scattering differences in specific regions of the reciprocal space for sarcoplasmic reticulum membranes containing protonated versus perdeuterated sarcoplasmic reticulum lipids which remain after scaling. (B), (C) Similar lamellar neutron diffraction from oriented sarcoplasmic reticulum membrane multilayers hydrated with 100% ^2H_2O containing either protonated (B) or deuterated (C) sarcoplasmic reticulum phosphatidylcholine incorporated via the phosphatidylcholine transfer protein catalyzed exchange reaction. The

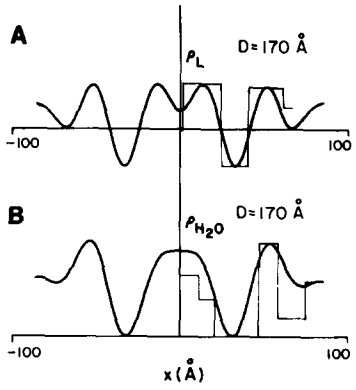

Fig. 4. The difference unit cell profile structure at low resolution (approx. 28 Å) calculated from the lamellar neutron diffraction of Fig. 3 which contains only the lipid profile structure of the two apposed sarcoplasmic reticulum (SR) membranes in the unit cell profile. The sarcoplasmic reticulum membrane lipid profile was calculated for an sarcoplasmic reticulum membrane multilayer with an average unit cell dimension of $D = 170$ Å. The unit cell water profile structure for sarcoplasmic reticulum membrane multilayers calculated from $H_2O/^2H_2O$ exchange ($D = 170$ Å) is shown in (B). Equivalent step-function model profiles are superimposed on a single-membrane profile (within $0 \leqslant |x| \leqslant D/2$) of the unit cell profile. The more obvious differences between the continuous unit cell sarcoplasmic reticulum membrane lipid and water profiles and their respective step-function model profiles for the single sarcoplasmic reticulum membrane arise from Fourier transform truncation effects.

monolayer of the sarcoplasmic reticulum lipid bilayer and therefore they also provide a direct evidence that the 'flip-flop' of exchanged phospholipid across the sarcoplasmic reticulum membrane profile had indeed reached equilibrium prior to the neutron diffraction experiments. The lipid profile asymmetry is somewhat more evident in the step-function model profile at this resolution. The ratio of the amount of water present within the outer versus the inner phospholipid headgroup region of the sarcoplasmic reticulum membrane profile was found to be 2.3 ± 0.2 (mean $\pm$ S.D.) as described in Methods.

strong scattering differences in specific regions of reciprocal space for sarcoplasmic reticulum membranes containing protonated versus perdeuterated PC are even greater than in (A) because the degree of PC perdeuteration was substantially greater in these particular experiments. Other differences in the scattered intensities for the experiments shown in (A) vs. (B, C) are the result of a different unit cell repeat (i.e. degree of hydration of the multilayer) for these two experiments.

(iii) Decomposition of the sarcoplasmic reticulum membrane electron density profile structure at approx. 12 Å resolution

The electron density profile structures of the intact sarcoplasmic reticulum membrane and the lipid bilayer of purified sarcoplasmic reticulum lipids at approx. 12 Å and approx. 15 Å resolution, respectively, previously determined [14] were placed on an absolute electron density scale as described in the Methods and are shown in Figs. 5A + inset. The corresponding separate lipid and protein profile structures within the sarcoplasmic reticulum membrane profile were obtained as described in Methods and are shown in Figs. 5B and 5C. The asymmetric lipid profile structure within the sarcoplasmic reticulum membrane (Fig. 5B) is shown placed on an absolute electron density scale to directly compare with the symmetric lipid profile structure (Fig. 5A, inset) obtained from highly purified sarcoplasmic reticulum lipids extracted from sarcoplasmic reticulum membranes. This profile structure which corresponds to the total lipid distribution within the sarcoplasmic reticulum membrane necessarily reflects the neutron diffraction result where more lipid was found in the inner versus the outer monolayer of the sarcoplasmic reticulum membrane lipid bilayer. The protein profile is shown as an area profile (Fig. 5C) to provide a more physically intuitive extension to the cylindrically-averaged protein structure (Fig. 5D) discussed below.

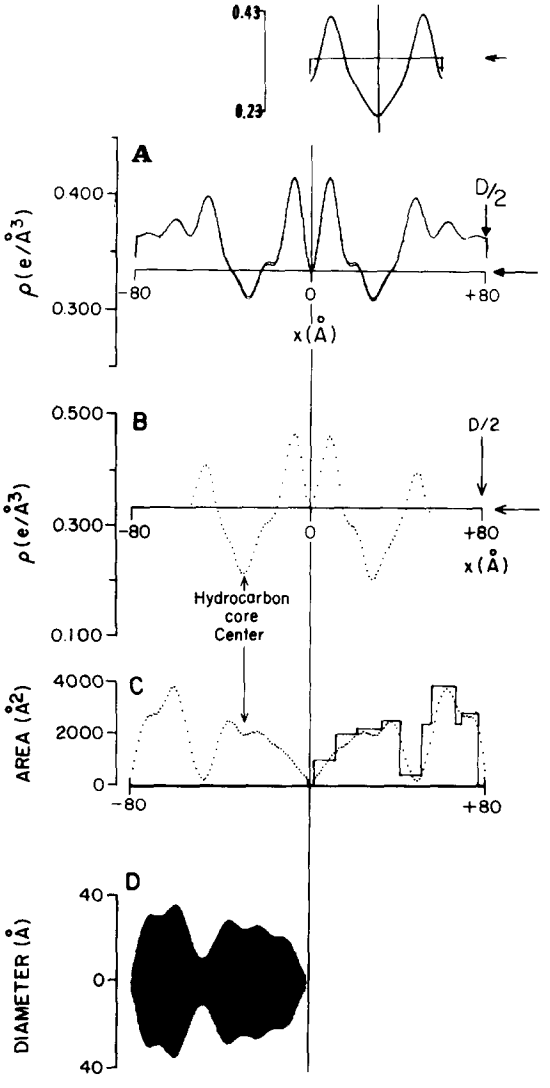

Fig. 5. (A) Electron density profile of the sarcoplasmic reticulum membrane taken from Herbette et al. [14] at approx. 11 Å resolution placed on an absolute electron density scale contained within $0 \leqslant |x| \leqslant D/2$ of the unit cell profile. The inset to (A) is the electron density profile of purified sarcoplasmic reticulum lipids ($D = 59$ Å) on an absolute electron density scale. (The electron density level of water is indicated by a horizontal arrow, $\rho = 0.334\ e/Å^3$). The direct decomposition of the sarcoplasmic reticulum membrane electron density profile into its lipid (B) and protein (C) profile structures at approx. 11 Å resolution obtained via model refinement calculations (see Methods) reflects the inequality in the number of phospholipid molecules in the outer versus inner monolayer of the sarcoplasmic reticulum lipid bilayer. The solid line superimposed on the protein profile for a single membrane within the unit cell ($0 < |x| < D/2$) in (C) represents the equivalent step-function model profile from which the continuous area profile structure (dotted line) was calculated. In (D) the cylindrically-averaged diameter of the calcium pump protein across the membrane profile as calculated from (C) is provided (see text).

The volume distributions of the total protein within the different regions of the sarcoplasmic reticulum profile structure were calculated from the area profile of Fig. 5C and are summarized in Table II. A comparison of the calculated volume of the calcium pump protein and the volume of this protein obtained in a separate neutron diffraction study of reconstituted sarcoplasmic reticulum which contains highly purified calcium pump protein [18] is summarized in Table III. Table III also provides some of the physical characteristics of the

TABLE II

VOLUME DISTRIBUTION OF TOTAL PROTEIN IN SARCOPLASMIC RETICULUM MEMBRANE

Region	Volume (Å^3)	% Volume [a]	% Volume [b]
Inner monolayer [c]	42600	27	–
Outer monolayer [c]	37400	24	–
Protein protrusion	77100	49	–
Total	157100	100	–
Hydrocarbon core	64200	40	
Inner monolayer (16 Å) [d]	32100 [d]	20	50
Outer monolayer (13 Å) [d]	32100 [d]	20	50
Protein protrusion [e]			
Inner 'knob'	50200	32	65
Outer 'knob'	26900	17	35

[a] Volume percent relative to total volume of calcium pump protein.

[b] Volume percent relative to total volume of protein in that region.

[c] Includes appropriate phospholipid headgroup region.

[d] Length of the average fatty acyl chain extension for each monolayer of the sarcoplasmic reticulum membrane bilayer which in turn implies that the protein occupies an area of 2000 Å^2 in the plane of the inner monolayer and an area of 2462 Å^2 in the plane of the outer monolayer.

[e] The electron density profile structure within $D/3 \leqslant |x| \leqslant D/2$ which is external to the membrane bilayer region contains two electron dense maxima. Inner 'knob' refers to that maximum in closest proximity to the outer phospholipid headgroup maximum while outer 'knob' refers to that maximum nearest $|x| = D/2$.

calcium pump protein obtained from this study in comparison to other experimental measurements.

(iv) Maximum profile extent of the sarcoplasmic reticulum membrane protein

Previous X-ray diffraction studies under the conditions of 20–30% water content for the sarcoplasmic reticulum membrane multilayer provided the electron density profile structure of the sarcoplasmic reticulum membrane to a resolution of approx. 11 Å (reproduced here on an absolute electron density scale, Fig. 5A). Under conditions of relatively low water content (i.e., 20% which appears to be the minimal amount of water which does not result in lipid phase separation of the sarcoplasmic reticulum membrane), X-ray diffraction of partially dehydrated-oriented multilayers of sarcoplasmic reticulum defines a unit cell profile dimension of 157 Å [14]. This unit cell profile has been shown to contain two highly asymmetric membrane profiles corresponding to the two apposed membranes of the flattened sarcoplasmic reticulum vesicle which is also convincingly supported by the pair of lipid bilayer profiles shown in Fig. 4A. The unit cell electron density profile reproduced in Fig. 5A shows that the separation between phospholipid headgroups within the single membrane profile is 40 Å and the sarcoplasmic reticulum membrane profile contains electron dense maxima just outside the outer monolayer phospholipid headgroup region at the extravesicular surface of the membrane. The actual mem-

TABLE III

PHYSICAL PARAMETERS OF THE Ca^{2+} PUMP PROTEIN

	Cross-sectional average area (Å^2)	Volume (Å^3)
Calculated	–	140000 [a]
SR model	2000	157100
Experimental	3000 [b]	162000 [c]
RSR model [d]	2700 [d]	160000

[a] Calculated from the known amino acid composition [41] and the partial specific volumes [47] of amino acid residues.

[b] Obtained from Inesi [11] utilizing the thickness of the sarcoplasmic reticulum (SR) bilayer obtained from previous X-ray diffraction studies [12,13] and the density measurement of the Ca^{2+} pump protein [48].

[c] Obtained from the measurement of the density of the Ca^{2+} pump protein utilizing CsCl density gradient centrifugation [48].

[d] Taken from Herbette et al. [18] for reconstituted sarcoplasmic reticulum (RSR).

brane width is very nearly equal to one-half of the unit cell profile dimension (i.e., approx. 75–77 Å) since the 'pure' water layers between neighboring unit cells are only a few ångstroms wide. Thus, under these conditions, it would appear that the sarcoplasmic reticulum membrane profile has a minimal width of 75–77 Å in the maximally 'compressed' multilayer.

Oriented multilayers of sarcoplasmic reticulum can, however, be swelled to relatively high water contents in the presence of $> 10\%$ sucrose in the multilayer water spaces yielding multilayer unit cell profile dimensions on the order of 200–270 Å depending on the sucrose concentration and total water content [13,14]. Under conditions of $< 10\%$ sucrose, we have observed multilayer unit cell profile dimensions on the order of 180–240 Å (approx. 30–40% water content). The single membrane profile width under these conditions is somewhat greater (86–88 Å) than that for multilayer unit cells in the 160–170 Å range as recently shown in the analysis of time-resolved X-ray diffraction data [43].

We have obtained X-ray scattering data from isolated unilamellar sarcoplasmic reticulum vesicular dispersions and calculated the single-membrane profile autocorrelation function, $Q_{exp}(x)$ (Fig. 6A). The 'average' membrane thickness, corresponding to the major non-origin peak in the autocorrelation function which is usually dominated by the phospholipid headgroup correlation across the membrane profile, was found to be 39 Å. This value correlates well with the separation of the electron dense maxima demonstrated to correspond to the phospholipid headgroups of the sarcoplasmic reticulum lipid bilayer within $0 \leqslant |x| \leqslant D/3$ of the electron density profile structure for the sarcoplasmic reticulum membrane reproduced in Fig. 5A, as obtained for an sarcoplasmic reticulum multilayer with minimal water content. The 'total' membrane thickness, corresponding to that value along the profile axis at which significant fluctuations in the autocorrelation function cease, is substantially greater, being 99 Å. Model refinement analysis of $Q_{exp}(x)$ as described in the Methods yielded a best-fit for $Q_{cal}(x)$ to $Q_{exp}(x)$ as shown in Fig. 6C based on the models of Fig. 6B. This best-fit corresponded to a single membrane profile structure in which the extravesicular surface maxima had a width of 40–50 Å (the total membrane width including the lipid bilayer was equal to approx. 100 Å). Thus, it would appear that since the phospholipid headgroup separation across the sarcoplasmic reticulum membrane profile structure is the same in vesicular dispersions and oriented multilayers, the protein protrusions from the extravesicular surface are rather 'elastic' protruding 20–50 Å from the sarcoplasmic reticulum lipid bilayer surface depending on the membrane's aqueous environment. This maximal sarcoplasmic reticulum membrane profile width in vesicular dis-

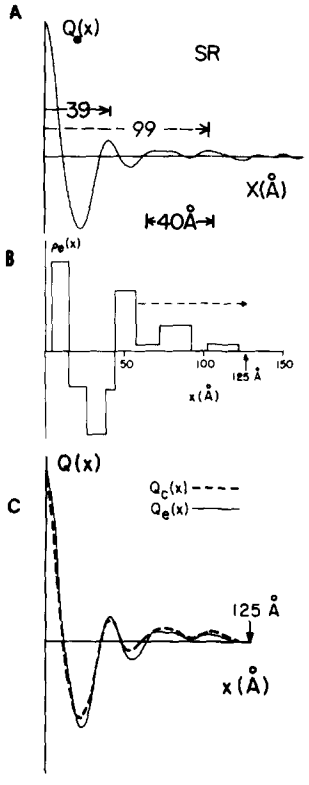

Fig. 6. (A) The autocorrelation function for the sarcoplasmic reticulum (SR) membrane profile. The solid line vector corresponds to the 'average' membrane thickness; the dotted line vector corresponds to the total membrane thickness (see text for a description of the terms 'average' and 'total' membrane thickness). Calculation (C) of the single membrane autocorrelation function (Q_{cal}) for the best fit to the experimentally determined autocorrelation function (Q_{exp}) based on the membrane model profiles shown in (B). The dotted line vector in (B) represents the profile extent of electron density that was varied to obtain the single membrane profile whose autocorrelation function gave the best fit to the experimental data.

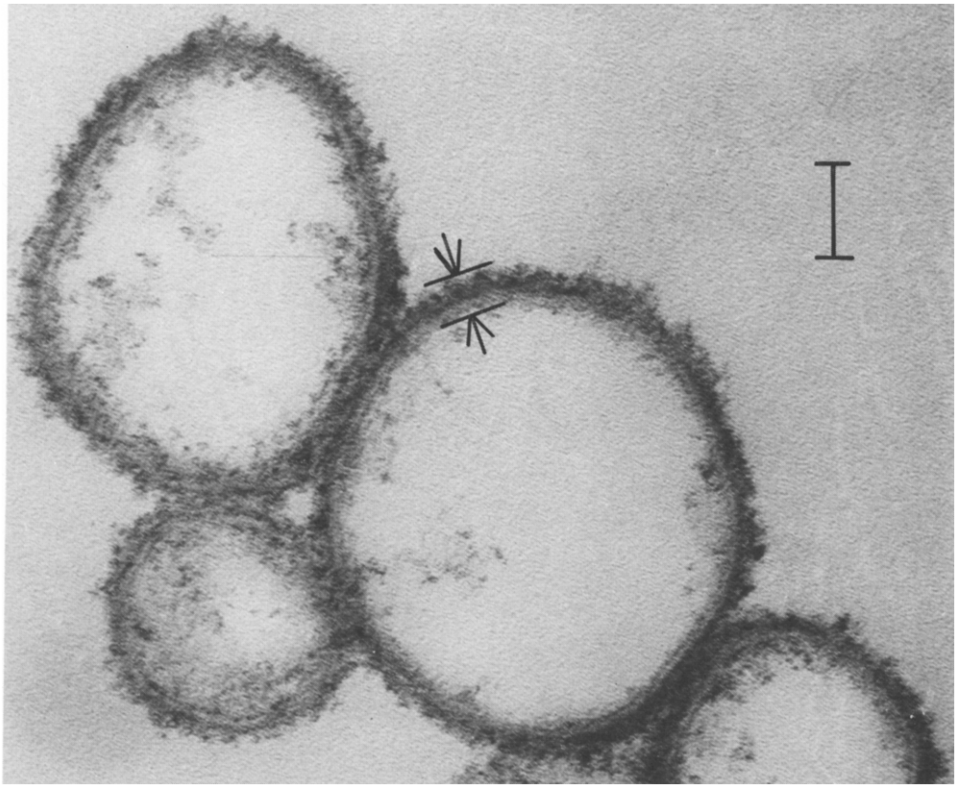

Fig. 7. High-magnification, thin-section electron micrograph of the sarcoplasmic reticulum membrane fixed with tannic acid and osmium. The arrowheads indicate that the approximate width of the membrane profile is approx. 90 Å. The bar represents 0.02 μm.

persions correlates well with the high-resolution thin-section electron microscopic image of the sarcoplasmic reticulum membrane shown in Fig. 7.

Discussion

Nature of the protein profile structure of the sarcoplasmic reticulum membrane

The calcium pump constitutes 90% of the protein in the sarcoplasmic reticulum membrane preparations utilized in this study [23,24]. The studies described provide the variation in the overall shape of the total protein present in these sarcoplasmic reticulum membranes over the different regions of the membrane profile as cylindrically-averaged about the normal to the membrane plane. In Fig. 5D, the total cross-sectional area occupied by protein (excluding water of hydration, etc.) is plotted as a function of the profile coordinate along the normal to the sarcoplasmic reticulum membrane plane. From this protein area profile structure, the cylindrically-averaged schematic in Fig. 8 was simply obtained. We note that since this protein area profile specifically excludes water, the actual area profile of the hydrated protein in regions of the membrane profile containing water (i.e., outside the hydrocarbon core region of the lipid bilayer within the sarcoplasmic reticulum membrane profile) may be somewhat greater. This cylindrically-averaged protein model given with some fine structure (12 Å resolution) in Fig. 8 can be treated roughly as a cylinder of approximately 60 Å diameter within the lipid bilayer of the sarcoplasmic reticulum membrane and a cylinder of approx. 80 Å diameter protruding from the extravesicular surface of the sarcoplasmic reticulum membrane bilayer. This picture for the cylindrically-averaged protein shape situated within the isolated sarcoplasmic reticulum membrane structure has features somewhat similar to that obtained for the deter-

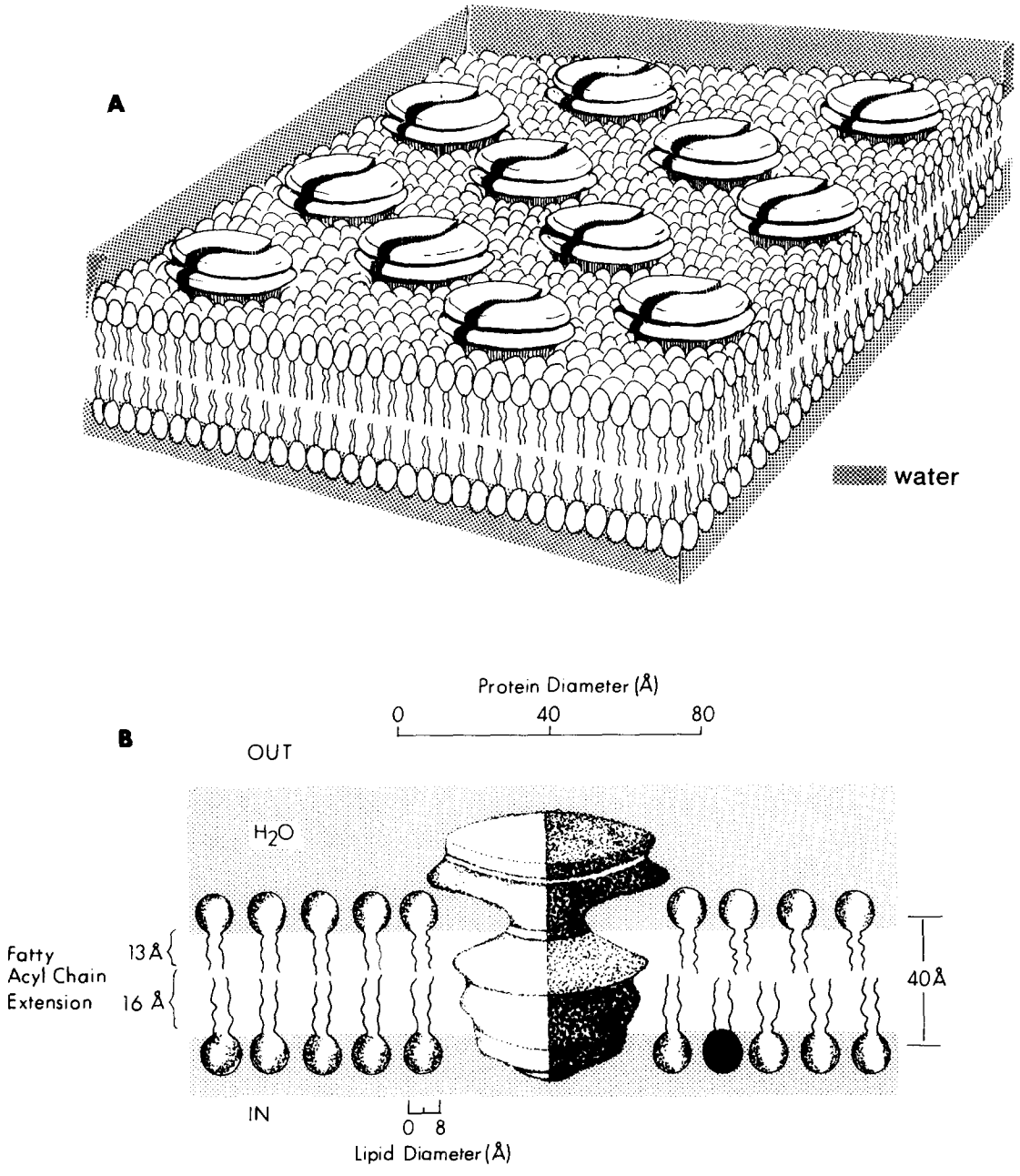

Fig. 8. Schematic representation of the structural organization of the sarcoplasmic reticulum membrane obtained by X-ray and neutron diffraction studies. In (A) the calcium pump protein molecules are assembled in the sarcoplasmic reticulum lipid bilayer with an average center to center separation of approx. 110–125 Å in the membrane plane [20]. In (B) a cross-sectional slice (parallel to the profile axis) through the calcium pump protein of the sarcoplasmic reticulum membrane depicting the cylindrically averaged protein shape and phospholipid dimensions. A darkened phospholipid molecule in the inner monolayer represents the additional lipid on the intravesicular side of the membrane.

gent-solubilized sarcoplasmic reticulum protein by LeMaire et al. [17]. We note that the cross-sectional area of protein averaged over the entire profile structure is similar to estimates based on the thickness of the sarcoplasmic reticulum membrane and the density of the calcium pump protein (see Table III).

The volume distribution of protein for different regions of interest within the sarcoplasmic reticulum membrane profile (Table II) can be directly calculated from the area profile of Fig. 5D. We define four regions of the single sarcoplasmic reticulum membrane (half unit cell) profile as follows: (1) The inner monolayer of the sarcoplasmic reticulum membrane lipid bilayer is defined as the region including the inner phospholipid headgroup maximum of the electron density profile (Fig. 5A) up to the center of the lowest density region in this profile structure; (2) The outer monolayer is the region from the center of this lowest density region up to and including the outer phospholipid headgroup maximum; (3) The regions external to the lipid bilayer of the sarcoplasmic reticulum membrane profile contain the protein protrusions from the bilayer's surface; and (4) the hydrocarbon core region of the sarcoplasmic reticulum membrane lipid bilayer occurs between (and not including) the phospholipid headgroups. 49% of the protein volume (mass) is located external to the lipid bilayer of the sarcoplasmic reticulum membrane protruding only from the outer extravesicular bilayer surface with 24% in the outer and 27% in the inner monolayer of the sarcoplasmic reticulum membrane lipid bilayer. Approximately 40% of the total protein is present in the hydrocarbon core (excluding the phospholipid headgroup regions) of the sarcoplasmic reticulum membrane lipid bilayer. This mass distribution is similar to that obtained by peptide sequence modeling of the sarcoplasmic reticulum calcium pump protein in which 60% of the total amino acid content was calculated to be external to the hydrocarbon core of the sarcoplasmic reticulum lipid bilayer [44].

The calculated volume for the total protein in our sarcoplasmic reticulum membrane preparations is similar to that obtained for both reconstituted sarcoplasmic reticulum where > 95% of the protein is the calcium pump [18] and the theoretical minimum volume calculated from the known amino acid composition of the calcium pump and their corresponding molecular volumes (Table III). This value for the total protein volume is, however, smaller than that obtained by LeMaire et al. [17] for detergent solubilized sarcoplasmic reticulum protein (182000 $Å^3$). The origin of non-calcium pump protein in the sarcoplasmic reticulum membrane that may explain this discrepancy is not known but could be a protein which binds tightly to the proteinaceous protrusions from the sarcoplasmic reticulum membrane's external surface. For example, MacLennan et al. [45] observed that a 53000 M_r protein does bind tightly to the sarcoplasmic reticulum in less purified isolated membrane fragments. The value obtained by Brady et al. [16] is somewhat lower (141000 $Å^3$) than our determination, but reasonably consistent with our results.

The length of the calcium pump protein along the profile axis is approx. 80 Å in a compressed multilayer and up to approx. 100 Å in dispersions of sarcoplasmic reticulum vesicles. Of this total profile extension, the protein protrusion from the sarcoplasmic reticulum membrane extravesicular surface is a particularly curious aspect of its structure. If the average density of the protrusion and hence its volume (77100 $Å^3$) is the same in dispersions as in a membrane multilayer, then the 40–50 Å profile extension of the protrusion in dispersions versus 25 Å in the multilayer defines an average cross-sectional area of 4000 $Å^2$ for the protrusion in the multilayer versus 2000 $Å^2$ in dispersion. The structure of the sarcoplasmic reticulum membrane within the lipid bilayer region of the membrane profile appears to be conserved in multilayers and dispersions of sarcoplasmic reticulum, based on the results given in Fig. 6. Thus the sarcoplasmic reticulum membrane width varies only with the extension of the protein protrusions from the membrane's extravesicular surface (Fig. 9A, B). The conformation of this 'elastic' component of the sarcoplasmic reticulum membrane profile apparently is not a strict requirement for calcium translocation since these oriented multilayers function as well as vesicle dispersions [46].

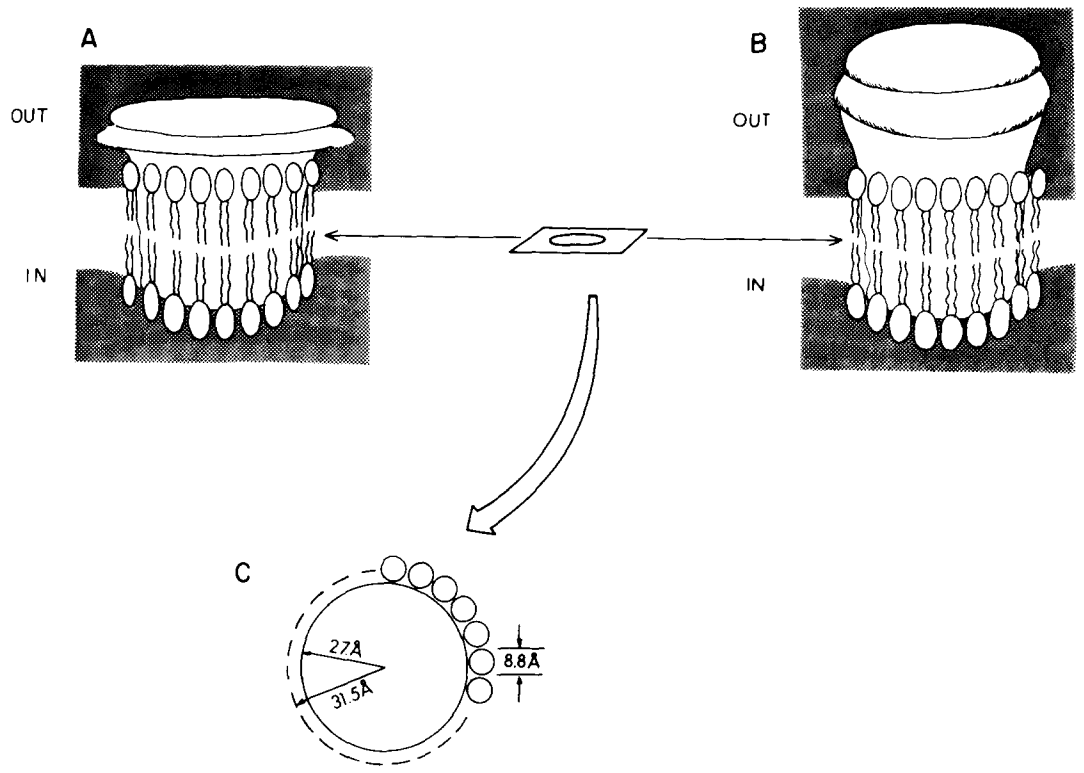

Fig. 9. Perspective drawing of the calcium pump protein in the sarcoplasmic reticulum membrane lipid bilayer. The protein protruding from the extravesicular surface of the sarcoplasmic reticulum membrane lipid bilayer is depicted in (A) for sarcoplasmic reticulum 'compressed' in a multilayer; in dispersion this protruding protein apparently has a maximal extension as shown in (B). Since the protein mass distribution within the membrane bilayer region of the sarcoplasmic reticulum membrane profile is similar for sarcoplasmic reticulum in dispersions and multilayers, the total mass of protein protruding from the extravesicular surface for both (A) and (B) must be similar. Based on the average cross-sectional area of the calcium pump protein within the membrane bilayer region, the first shell of annular lipids was calculated to contain 45 phospholipid molecules which comprises 35–45% of the total phospholipid of the sarcoplasmic reticulum membrane (C). Shaded area indicates water.

Origin of asymmetry in the sarcoplasmic reticulum membrane electron density profile-lipid profile structure

The asymmetry in the electron density profile of the sarcoplasmic membrane arises from two sources. The first and major contribution to this highly asymmetric membrane profile is obviously the result of approximately 50% of the protein mass being located externally on only one surface of the sarcoplasmic reticulum membrane lipid bilayer. The second and more subtle source of asymmetry arises from the distributional asymmetry of lipid and hence protein between the two apposed lipid monolayers of the sarcoplasmic reticulum membrane bilayer which, together with the ratio of water hydrating the outer versus the inner phospholipid headgroup regions, are the apparent bases for the difference in the amplitudes of the major electron dense maxima within the lipid bilayer region, $0 \leqslant |x| \leqslant D/3$, of the sarcoplasmic reticulum membrane profile structure (Fig. 5A). Thus, we define compositional asymmetry as the inequality in the distribution or number of lipid molecules between the outer and inner monolayers of the sarcoplasmic reticulum lipid bilayer. In addition to this compositional asymmetry for the lipid component of the sarcoplasmic reticulum membrane, the higher-resolution model refinement of the electron density profile also shows that the average fatty-acyl chain extension in the inner monolayer is approx. 20% greater than in the outer monolayer (conformational asymmetry). The com-

positional and conformational asymmetries of the sarcoplasmic reticulum lipid bilayer must be the result of the calcium pump protein present within this bilayer (see footnote d, Table II).

Apart from the fine details regarding the origin of asymmetry in the electron density profile structure of the sarcoplasmic reticulum membrane, the roughly cylindrical shape of the calcium pump protein throughout the membrane lipid bilayer region does allow a calculation of the number of lipid molecules that could be in direct contact with the pump protein. As shown in Fig. 9C, a simple geometrical argument predicts that approximately 45 phospholipids are in direct contact with the calcium pump protein. Given that the structure of the sarcoplasmic reticulum membrane within the lipid bilayer region appears to be similar for the sarcoplasmic reticulum vesicle dispersions and multilayers, this value of 45 phospholipids, as calculated, is referable to a single calcium pump protein molecule in both cases.

Relevance of the sarcoplasmic reticulum membrane structure to its function

The protein mass distribution in the sarcoplasmic reticulum membrane is seen to be highly asymmetric with 50% of the protein located external to the extravesicular surface of the sarcoplasmic reticulum membrane lipid bilayer. The remaining 50% of the protein mass, present within the sarcoplasmic reticulum membrane lipid bilayer, is distributed somewhat asymmetrically between the two monolayers (see footnote d, Table II). The total phospholipid distribution is also seen to be asymmetric with more lipid in the inner monolayer. This complementary asymmetry of the protein and lipid components within the lipid bilayer region of the sarcoplasmic reticulum membrane profile preserves the combined average cross-sectional area for the lipid and protein across the sarcoplasmic reticulum membrane profile allowing for the unidirectional incorporation of a highly asymmetric protein structure into the lipid bilayer, and hence, the vectorial translocation of calcium across the membrane profile.

Static structure of the sarcoplasmic reticulum membrane related to its dynamic structure

The detailed structural picture of the sarcoplasmic reticulum membrane described here corresponds to the functional state of this membrane prior to calcium transport. Possible changes in the sarcoplasmic reticulum membrane profile structure associated with various functional states occurring during ATP-induced calcium transport [43] are being investigated utilizing synchrotron radiation sources in time-resolved X-ray diffraction studies. The interpretation of these time-resolved results depends critically on knowing the detailed structure of the separate components of the sarcoplasmic reticulum membrane prior to ATP-induced calcium transport. The combined X-ray and neutron diffraction approach described here thus provides a reference frame for interpreting the dynamic structure of the sarcoplasmic reticulum membrane during active calcium transport.

Comment on the 'direct difference' approach

The 'direct difference' approach utilized provides essential information in order for the model refinement analysis to converge to a unique solution. When strong constraints (such as the direct determination of the water and lipid profile structures within the membrane profile structure) are placed on the model refinement approach, the correct protein profile structure can be obtained. We note that the 'direct difference' approach employed here is the first direct determination of the profile structures of the separate lipid and protein components within an isolated biological membrane.

Acknowledgements

This work was supported by grants from the NIH (HL-27630, HL-32588) and the American Heart Association (with partial support by the Connecticut affiliate) (to L.H), the NIH AM-14632 and a Muscular Dystrophy Assocation of America grants (to S.F.), and an NIH grant HL-18708 (to J.K.B. and A.S.). L. Herbette is a Charles E. Culpeper Foundation Fellow.

References

1 Inesi, G. (1979) Membrane Transport in Biology, pp. 357–393, Springer-Verlag, Berlin
2 Tada, M., Yamamoto, T. and Tonomura, Y. (1978) Physiol. Rev. 58, 1–79

3 Hasselbach, W. (1978) Biochim. Biophys. Acta 515, 23–53
4 Ikemoto, N. (1982) Annu. Rev. Physiol. 44, 297–317
5 Scales, D. and Inesi, G. (1976) Biophys. J. 16, 735–751
6 Deamer, D.W. and Baskin, R.J. (1969) J. Cell. Biol. 43, 610–617
7 Inesi, G. and Asai, H. (1968) Arch. Biochem. Biophys. 126, 469–477
8 Kalina, M. and Pease, D.C. (1977) J. Cell. Biol. 74, 726–741
9 Kalina, M. and Pease, D.C. (1977) J. Cell. Biol. 74, 742–746
10 Saito, A., Wang, C.T. and Fleischer, S. (1978) J. Cell. Biol. 79, 601–616
11 Inesi, G. (1972) Annu. Rev. Biophys. Bioeng. 1, 191–210
12 DuPont, Y., Harrison, S.C. and Hasselbach, W. (1973) Nature (Lond.) 244, 555–558
13 Worthington, C.R. and Liu, S.C. (1973) Arch. Biochem. Biophys. 157, 573–579
14 Herbette, L., Marquardt, J., Scarpa, A. and Blasie, J.K. (1977) Biophys. J. 20, 245–272
15 Herbette, L., Wang, C.T., Saito, A., Fleischer, S., Scarpa, A. and Blasie, J.K. (1981) Biophys. J. 36, 47–72
16 Brady, G.W., Fein, D.B., Harder, M.E. and Meissner, G. (1982) Biophys. J. 37, 637–645
17 LeMaire, M., Moller, J.V. and Tardieu, A. (1981) J. Mol. Biol. 150, 273–296
18 Herbette, L., Scarpa, A., Blasie, J.K., Wang, C.T., Hymel, L., Seelig, J. and Fleischer, S. (1983) Biochim. Biophys. Acta 730, 369–378
19 Blasie, J.K., Pachence, J.M. and Herbette, L.G. (1983) Brookhaven Symposium, Neutron Scattering in Biology
20 Napolitano, C.A., Cooke, P., Segalman, S. and Herbette, L. (1983) Biophys. J. 42, 119–125
21 Hymel, L., Maurer, A., Berenski, C., Jung, C. and Fleischer, S. (1984) J. Biol. Chem. 259, 4890–4895
22 Herbette, L. and Blasie, J.K. (1980) Calcium-Binding Proteins: Structure and Function, pp. 115–120, Elsevier-North Holland, Amsterdam
23 Meissner, G., Conner, G.E. and Fleischer, S. (1973) Biochim. Biophys. Acta 298, 246–269
24 Meissner, G. (1975) Biochim. Biophys. Acta 389, 51–68
25 Wang, C.T., Saito, A. and Fleischer, S. (1979) J. Biol. Chem. 254, 9209–9219
26 Lowry, O.H., Rosebrough, N.J., Farr, A.L. and Randall, R.J. (1951) J. Biol. Chem. 193, 265–275
27 Meissner, G. and Fleischer, S. (1971) Biochim. Biophys. Acta 241, 356–378
28 Crain, R.C. and Zilversmit, D.B. (1980) Biochemistry 19, 1433–1439
29 Zilversmit, D.B. (1983) Methods Enzymol. 98, 565–573
30 North, P. and Fleischer, S. (1983) J. Biol. Chem. 258, 1242–1253
31 Kamp, H.H., Wirtz, K.W.A. and Van Deenen, L.L.M. (1973) Biochim. Biophys. Acta 318, 313–325
32 North, P. and Fleischer, S. (1984) Biochim. Biophys. Acta 772, 65–76
33 Pachence, J.M., Dutton, P.L. and Blasie, J.K. (1981) Biochim. Biophys. Acta 635, 267–283
34 Schwartz, S., Cain, J.E., Dratz, E.A. and Blasie, J.K. (1975) Biophys. J. 15, 1201–1233
35 Moody, M.F. (1963) Science (Wash. D.C.) 142, 1173–1174
36 Stamatoff, J.B. and Krimm, S. (1976) Biophys. J. 16, 503–516
37 Guiner, A. (1963) X-ray Diffraction, W.H. Freeman, San Francisco, CA
38 Buldt, G., Gally, H.U., Seelig, J. and Zaccai, G. (1979) J. Mol. Biol. 134, 673–691
39 Pachence, J.M., Dutton, P.L. and Blasie, J.K. (1979) Biochim. Biophys. Acta 548, 348–373
40 Levine, Y.K. (1973) Progress in Surface Science, Pergamon Press, Elmsford, New York
41 MacLennan, D.H., Seeman, P., Iles, G.H. and Yip, C.C. (1971) J. Biol. Chem. 246, 2702–2710
42 Blaurock, A.E. (1972) Adv. Exp. Med. Biol. 24, 53–63
43 Blasie, J.K., Herbette, L.G., Pascolini, D., Skita, V., Pierce, D.H. and Scarpa, A. (1985) Biophys. J., in the press
44 MacLennan, P.H., Reithmeier, R.A.F., Shoshan, V., Campbell, K.P., Lebel, D., Herrman, T.R. and Shamoo, A.E. (1980) Ann. N.Y. Acad. Sci. 358, 138–148
45 MacLennan, D.H. (1974) Methods Enzymol. 32, 291–302
46 Pierce, D.H., Scarpa, A., Trentham, D.R., Topp, M.R. and Blasie, J.K. (1983) Biophys. J. 44, 365–373
47 Cohn, E.J. and Edsall, J.T. (1943) Proteins, Amino Acids and Peptides, Reinhold, New York
48 McFarland, B.H. and Inesi, G. (1971) Arch. Biochem. Biophys. 145, 456–464